



ELSEVIER

Contents lists available at ScienceDirect

Journal of Magnetism and Magnetic Materials

journal homepage: www.elsevier.com/locate/jmmmField induced phase transitions on NdRhIn₅ and Nd₂RhIn₈ antiferromagnetic compoundsJ.G.S. Duque^{a,*}, R. Lora Serrano^b, D.J. Garcia^c, L. Bufaical^d, L.M. Ferreira^d, P.G. Pagliuso^d, E. Miranda^d^a Núcleo de Física, Campus Itabaiana, UFS, 49500-000 Itabaiana, SE, Brazil^b Instituto de Física, Universidade Federal de Uberlândia, 38400-902 Uberlândia-MG, Brazil^c Consejo Nacional de Investigaciones Científicas y Técnicas (CONICET) and Centro Atómico Bariloche, S.C. de Bariloche, Río Negro, Argentina^d Instituto de Física "Gleb Wataghin", UNICAMP, 13083-970 Campinas-São Paulo, Brazil

ARTICLE INFO

Article history:

Received 7 September 2010

Received in revised form

21 October 2010

Available online 24 November 2010

Keywords:

Antiferromagnetic
Magnetic transition
Susceptibility

ABSTRACT

In this work, we have investigated the low temperature magnetic phase diagram of the tetragonal NdRhIn₅ and Nd₂RhIn₈ single crystals by means of temperature and field dependent heat capacity and magnetic susceptibility measurements. These compounds order antiferromagnetically with a Néel temperature (T_N) of 11 and 10.7 K for NdRhIn₅ and Nd₂RhIn₈, respectively. The constructed magnetic phase of both compounds are anisotropic and show, as expected, a decrease of T_N as a function of the magnetic field for c crystallographic direction. However when the magnetic field is applied along of the c -axis, which is the magnetic easy axis, first-order-like field induced transitions are observed within the antiferromagnetic state. We compare the phase diagrams obtained for NdRhIn₅ and Nd₂RhIn₈ with those for their cubic relative NdIn₃.

© 2010 Elsevier B.V. All rights reserved.

1. Introduction

Nd_{*m*}Rh_{*n*}In_{3*m*+2*n*} ($n=0, 1; m=1, 2$) are tetragonal compounds variants of the Cu₃Au-structure [1–6]. Their structure can be viewed as m layers of RIn₃ units sequentially stacked along the c -axis with n layers of MIn₂. It is well known that Ce-based heavy fermion compounds exhibit an unusual coexistence of antiferromagnetic (AF) and superconductivity (SC) at ambient pressure or high pressures [7,8], in which both AF and SC are believed to arise from 4*f* electrons. A magnetic mediation of the pairing mechanism has been argued for these novel compounds [7]. However, there are still many unsolved questions in this unique group of materials to be further clarified. It has been suggested that the reduced spatial dimensionality and magnetic anisotropy resulting from the quasi-2D structure of these compounds may control the nature of their heavy-fermion ground states [1,6]. Therefore, studies in non-Kondo isostructural magnetic materials of the same R_{*m*}M_{*n*}In_{3*m*+2*n*} series may be useful in understanding the role of spatial dimensionality, magnetic anisotropy, and crystal field effects in the evolution of the magnetic properties within these series. The variety of interesting physical properties in structurally related series represent a great opportunity to explore systematically the role of the Ruderman–Kittel–Kasuya–Yoshida (RKKY) magnetic interaction, Kondo effect, crystalline electrical field (CEF), Fermi surface (FS) effects in determining their properties, specially, in

favoring unconventional superconductivity (USC) in many Ce-based members of these series [4,5,9–11]. As the Pr-based homologues are non-magnetic singlet ground state systems [1], the Nd-based materials are the obvious candidates for such a study.

2. Experiment

Single crystalline samples of the Nd_{*m*}Rh_{*n*}In_{3*m*+2*n*} ($n=0, 1; m=1, 2$) were grown from the melt in In flux as described previously [1]. Typical crystal sizes were 1 × 1 cm × several mm. The tetragonal HoCoGa₅ ($m=1$) and Ho₂CoGa₈ ($m=2$) [12,13] structure types and phase purity were confirmed by X-ray powder diffraction, and the crystal orientation was determined by the usual Laue method. Specific-heat measurements were performed in a small-mass calorimeter that employs a quasiadiabatic thermal relaxation technique. Samples used here ranged from 10 to 30 mg. Magnetization measurements were made in a quantum design dc superconducting quantum interference device and in a physical properties measurement system (quantum design) in the temperature range $2 \leq T \leq 20$ K.

3. Results and discussion

Fig. 1 shows magnetic contribution to the specific heat divided by temperature to (a) NdRhIn₅ and (b) Nd₂RhIn₈ to different values of applied magnetic field along c -axis of the samples. The inset of Fig. 1 presents magnetic specific heat measured at $H=90$ kOe. To

* Corresponding author.

E-mail address: gerivaldoduque@gmail.com (J.G.S. Duque).

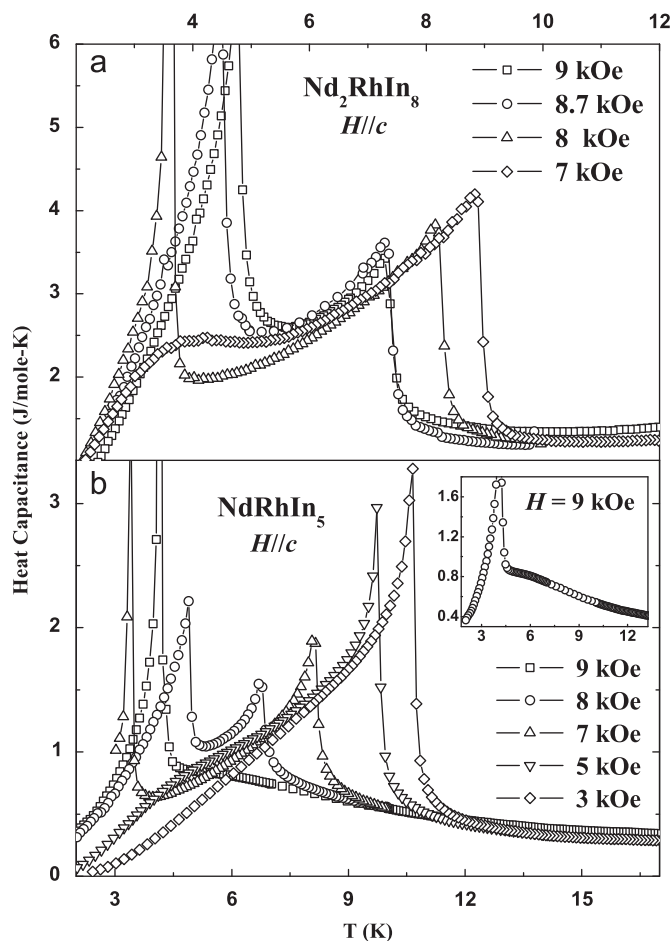


Fig. 1. Magnetic specific heat of (a) NdRhIn₅ and (b) Nd₂RhIn₈ at different values of applied magnetic field along *c*-axis of the samples.

obtain the magnetic contribution to the specific heat, the phonon contribution was subtracted from the original data using the specific heat data of LaRhIn₅ and La₂MIn₈. For all data the peak at higher temperature range is consistent with the onset of antiferromagnetic order, which is continuously suppressed for increasing the magnetic field. Besides, an additional peak (first-order-like to $H > 70$ kOe) can be observed at lower temperature range.

It has been shown [14–16] via magnetization measurements that the cubic compound NdIn₃ is an antiferromagnet with $T_N \approx 6$ K. Magnetic order develops in a Γ_8 quartet crystal field ground state with [0 0 1] being the easy axis [15]. The insertion of M–In layers along the *c*-axis in NdRhIn₅ and Nd₂RhIn₈ causes the Néel temperatures to increase by a factor of 2 [5]. In a similar way the application of a magnetic field to the tetragonal relatives NdRhIn₅ and Nd₂RhIn₈ gives rise also to an additional magnetic transition inside the ordered state as one can see in the magnetic specific heat data shown in Fig. 1. The evolution in T_N can be explained qualitatively by the character of the crystal field ground state and the extent to which it is isolated, that is, experimental data results suggest that T_N is increased by the splitting of the Γ_8 quartet ground state into two doublets for the less symmetric variants and also that T_N increases with increasing doublet–doublet splitting. Indeed, Hieu et al. [17] have shown in a recent paper that a Γ_8 quartet crystal field ground state in the NdIn₃ spites in two doublets in the NdRhIn₅ compound.

The suppression of the order temperature as function of the magnetic field is accompanied with the appearance of a low temperature peak. At $H=90$ kOe the order temperature is completely suppressed and only that low temperature peak (with first-order-like

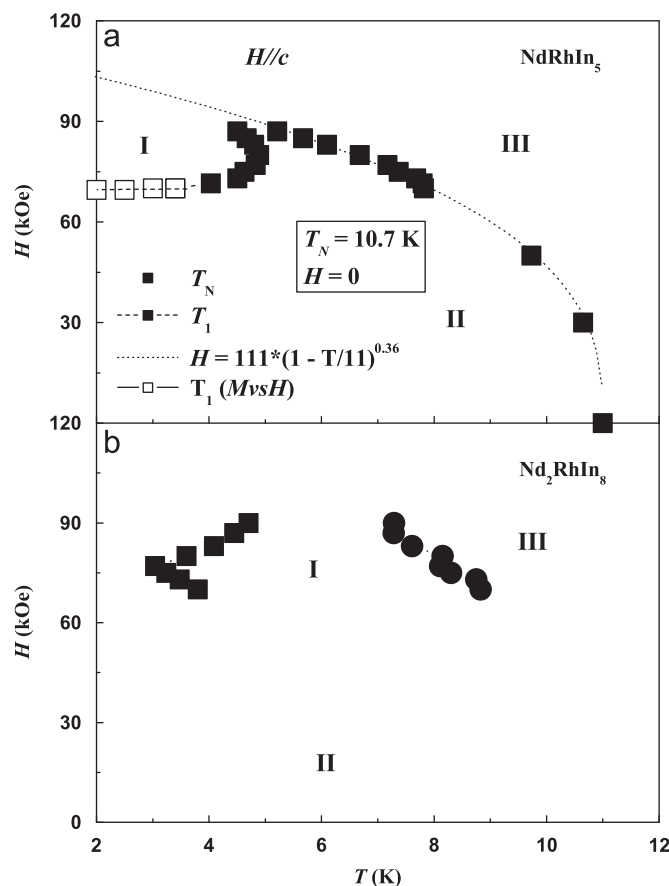


Fig. 2. The cumulative phase diagrams for (a) NdRhIn₅ and (b) Nd₂RhIn₈ for various applied fields applied along the *c*-axis. T_N corresponds to the antiferromagnetic ordering temperature and T_1 corresponds to field-induced transition.

character) is observed (see inset in Fig. 1). Fig. 2 summarize our experimental data through the cumulative phase diagrams for NdRhIn₅ and Nd₂RhIn₈ for various applied fields applied along the *c*-axis. T_N corresponds to the antiferromagnetic ordering temperature and T_1 corresponds to field-induced transition.

The magnetic phase diagram constructed via specific heat data is very similar to that observed by Hieu et al. [18] to the NdRhIn₅ compound using high-field magnetization measurements. Similar phase diagrams have also been observed for them to the family RRhIn₅ (R=Tb, Dy and Ho). The pointed line is the best fit to the expression $H = H_0(1 - T/T_N)^\beta$, $H_0 = 111$ kOe; $T_N = 11$ K and $\beta = 0.36$.

Below $T_N \approx 6$ K, the cubic relative NdIn₃ show two additional antiferromagnetic transitions at 4.61 and 5.13 K. The resulting complex magnetic phase diagram with metamagnetic processes arises due to the presence of crystal field and magneto-elastic effects and both bilinear and quadrupolar exchange interactions [15,19,16,20]. These two intermediate phases were determined to have incommensurate structures with magnetic propagation vectors $q_M = (1/2 \ 0.037 \ 1/2)$ and $(1/2 \ 0.017 \ 1/2)$, respectively, while the ground state structure was determined to be commensurate with $q_M = (1/2 \ 0 \ 1/2)$ and staggered Nd moments of approximately $2.0\mu_B$ with [0 1 0] the easy magnetization direction [21,15].

On the other hand, neutron diffraction experiments performed to the NdRhIn₅ at $T < T_N$ reveal that the ground-state magnetic structure was found to be a commensurate antiferromagnetic structure with a magnetic wave vector $q_M = (1/2 \ 0 \ 1/2)$ [22]. Therefore, ground-state magnetic structure of NdRhIn₅ suggests that the insertion of a RhIn₂ layer creates a commensurate magnetic structure more robust and stable in the tetragonal

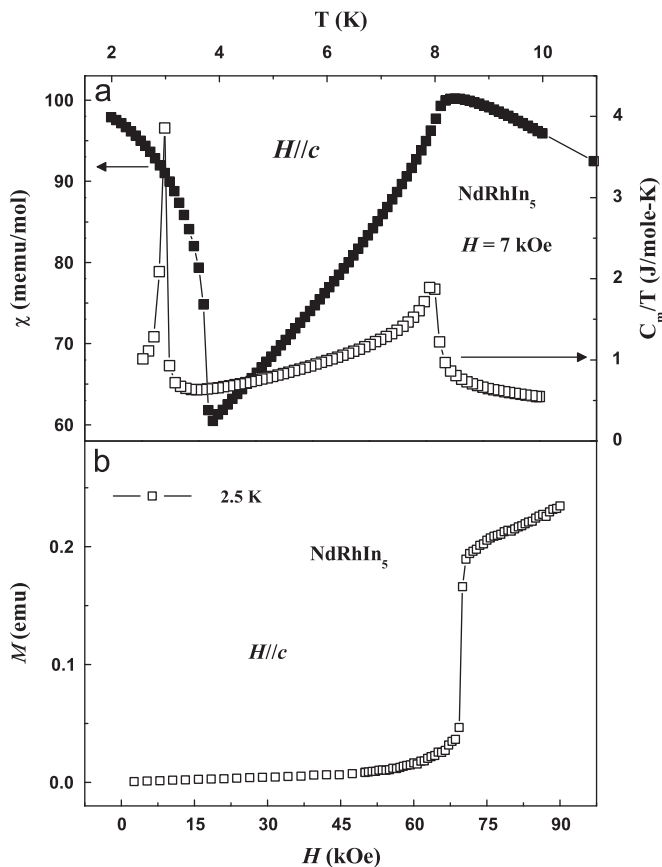


Fig. 3. Magnetization measurements as function of (a) temperature to $H=70$ kOe and (b) magnetic field to selected temperatures values along c -axis of NdRhIn₅ sample. We show that the magnetic susceptibility together with the magnetic specific heat performed at $H=70$ kOe.

variant. Indeed, the Nd^{3+} ($J=9/2$) ion in axial symmetry commonly has its multiplet split in anisotropic doublets (with $g_c \gg g_{\perp}$) favoring the Nd spins to point along the c -axis which is consistent with our results.

As one can see that complex behavior shown by NdIn₃ also seems to occur to NdRhIn₅ and Nd₂RhIn₈ relatives compounds as function of an applied magnetic field. The magnetic phase diagram is clearly separated in three regions: I, II and III. At low magnetic field (region I) the commensurate antiferromagnetic structure with a magnetic wave vector $q_M=(1/2\ 0\ 1/2)$ [22] is still observed. With increasing magnetic fields, metamagnetic processes give rise to a new magnetic structures (see Ref. [18]) due to the competition among the different inter and intra-layer exchange constants (regions II and III).

Fig. 3 present magnetization measurements as function of (a) temperature to $H=70$ kOe and (b) magnetic field at $T=2$ K along c -axis of NdRhIn₅ sample. We show together with the $MvsT$ curve the magnetic specific heat performed at $H=70$ kOe. Once magnetic susceptibility is performed along the easy direction (c -axis) the magnetic moment should decrease with decreasing temperature.

However, below T_N , one can see that the magnetic susceptibility decreases and in the onset of the field induced phase begins to increase. As we have commented above the increase in the magnetic susceptibility is related with the metamagnetic transition which occur inside the ordered state. In fact, Hieu et al. [18] have shown that the high-field magnetization presents two metamagnetic transitions at distinct values of magnetic field. In Fig. 3(b) we also show that our sample presents such sharp metamagnetic transition and it is consistent the field induced magnetic transition shown in the $MvsT$ and magnetic specific heat measurements.

4. Conclusions

In this work we measured the magnetic specific heat as function of the magnetic field for NdRhIn₅ and Nd₂RhIn₈ along the c -axis. The experimental data show that the Néel temperature is decreased for increasing the applied magnetic field and a field induced magnetic peak is observed inside the ordered state. At high fields this magnetic peak has a first-order-like character. A magnetic phase diagram was constructed through the specific heat measurements. It reflects the sharp two-step metamagnetic transition as one can see in the $MvsH$, $MvsT$ and magnetic specific heat measurements. For comparing the magnetic phase diagram of NdRhIn₅ and Nd₂RhIn₈ with its cubic relative NdIn₃ we conclude that a commensurate magnetic structure more stable is generated in the tetragonal variant.

Acknowledgments

This work was supported by FAPESP and CNPq, Brazil.

References

- [1] H. Hegger, et al., Phys. Rev. Lett. 84 (2000) 4986.
- [2] C. Petrovic, et al., Europhys. Lett. 53 (2001) 354.
- [3] C. Petrovic, et al., J. Phys.: Cond. Matter 13 (2001) L337.
- [4] P.G. Pagliuso, et al., Phys. Rev. B 63 (2001) 054426.
- [5] P.G. Pagliuso, et al., Phys. Rev. B 62 (2000) 12266.
- [6] J.D. Thompson, et al., J. Magn. Magn. Mater. 226–230 (2001) 5.
- [7] N.D. Mathur, et al., Nature (London) 394 (1998) 39.
- [8] E. Bauer, et al., Phys. Rev. Lett. 92 (2004) 027003.
- [9] E. Granado, et al., Phys. Rev. B 74 (2006) 214428.
- [10] E. Granado, et al., Phys. Rev. B 69 (2004) 144411.
- [11] R. Lora-Serrano, et al., Phys. Rev. B 74 (2006) 214404.
- [12] Y.N. Grin, et al., Sov. Phys. Crystallogr. 24 (1979) 137.
- [13] Y.N. Grin, et al., J. Less-Common Met. 121 (1996) 497.
- [14] K.H.J. Buschow, H.W. de Wijn, M. Van Diepen, J. Chem. Phys. 50 (1969) 137.
- [15] M. Amara, R.M. Galera, P. Morin, T. Verez, P. Burlet, J. Magn. Magn. Mater. 130 (1994) 127; M. Amara, R.M. Galera, P. Morin, J. Voiron, P. Burlet, J. Magn. Magn. Mater. 131 (1994) 402; M. Amara, R.M. Galera, P. Morin, T. Verez, P. Burlet, J. Magn. Magn. Mater. 1157 (1994) 140.
- [16] A. Czopnik, et al., Phys. Status Solidi A 127 (1991) 243.
- [17] N.V. Hieu, et al., J. Phys. Soc. Jpn. 76 (2007) 064702.
- [18] N.V. Hieu, et al., J. Phys. Soc. Jpn. 75 (2006) 074708.
- [19] K.H.J. Buschow, et al., J. Chem. Phys. 50 (1969) 137.
- [20] A. Czopnik, et al., Physica B 130 (1985) 259.
- [21] S. Mitsuda, et al., J. Phys. Soc. Jpn. 61 (1992) 1469.
- [22] S. Chang, et al., Phys. Rev. B 66 (2002) 132417.